IJMSO

International Journal of Mathematical Sciences and Optimization: Theory and Applications
Vol. 9, No. 1, pp. 59 - 80
https://doi.org/10.5281/zenodo.8218009

Lie-group analysis of flow and heat transfer of a dissipating fluid past stretching/shrinking surfaces with variable viscosity and non-uniform heat flux

H. A. Isede[1*], A. Adeniyan[2], N. Ogbonna[3]

1,2 Department of Mathematics, University of Lagos, Akoka, Lagos State.
3 Department of Mathematics, Michael Okpara University of Agriculture, Umudike, Nigeria.
* Corresponding author: hisede@unilag.edu.ng

Article Info
Received: 13 June 2023 Revised: 16 July 2023
Accepted: 19 July 2023 Available online: 25 July 2023

Abstract

The effects of surface mass flux (suction/injection) and variable viscosity on free-forced convection along a stretching or shrinking permeable plate embedded in a saturated porous medium are investigated through Lie-group analysis for steady two-dimensional flow in this paper. Assumptions are made that the fluid viscosity varies as a linear function of temperature and the heat flux through the plate wall varies with power law of the distance from the edge of the plate in a thermally radiating and incompressible fluid. The governing equations are tackled by means of Lie-group scaling transformation as to obtain a system of ordinary differential equations. Using Runge-Kutta-Gill scheme along with the shooting iteration technique, the resultant boundary-value problem is integrated numerically for different values of the physical fluid flow parameters. Comparisons between other previously published works with the present study were carried out for special cases and excellent agreements were demonstrated. The effect of moderate Prandtl number for a shrinking sheet is to reduce not only the velocity and temperature of the fluid but also the wall temperature gradient. Findings reveal that the wall friction parameter (skin-friction coefficient) and local heat transfer rate (Nusselt number or inverse wall temperature) increase with viscosity variation parameter aside the significant dependence on other emerging flow controlling parameters.

Keywords: Lie-group analysis; porous medium; permeable wall; variable viscosity; viscous dissipation; heat flux.
MSC2010: 76D99.

IJMSO

International Journal of Mathematical Sciences and Optimization: Theory and Applications
Vol. 9, No. 1, pp. 59 - 80
https://doi.org/10.5281/zenodo.8218009

Table 1: Nomenclature of Symbols

Nomenclature

A viscosity variation parameter, [-]
u, v fluid velocity, [ms^{-1}]
Da Darcy number, [-]
F_w surface lateral mass flux parameter, [-]
Gr Grashof number, [-]
p fluid pressure, [Nm^{-2}]
x, y cartesian coordinates, [m]
T fluid temperature, [K]
T_∞ fluid ambient temperature, [K]
g acceleration due to gravity, [ms^{-2}]
C_p specific heat at fixed pressure, [$Jkg^{-1}K^{-1}$]
Pr Prandtl number, [-]
C_f skin friction, [-]
N_u Nusselt number, [-]
Nr thermal radiation parameter, [-]
q_w wall heat flux [Wm^{-2}]
k thermal conductivity [$Wm^{-1}K^{-1}$]
K_p permeability of the porous medium, [m^2]
k^* Rosseland mean absorption coefficient, [m^{-1}]
V_w mass flux transverse velocity, [ms^{-1}]
U_w mass flux axial velocity,[ms^{-1}]

Greek Letters

λ stretching parameter, [-]
μ fluid viscosity, [Nsm^{-2}]
ν_∞ kinematic viscosity far from the sheet, [m^2s^{-1}]
ρ fluid density, [kgm^{-3}]
θ dimensionless temperature, [-]
β volumetric expansion coefficient, [K^{-1}]
σ^* Stefan-Boltzmann constant [$Wm^{-2}K^{-4}$]
σ_s emission scattering coefficient [m^{-1}]

1 Introduction

Many a physical phenomenon involves free (natural) convection driven by buoyancy forces in conjunction with the influences of thermal radiation. Free convective boundary-layer flow near moving or stationary solid surfaces is a classical problem and has been extensively investigated and still receives serious attention in active research areas for the last few decades; dated back to the contracted investigation of [1]. Obvious reasons are adduced to perceived industrial and technological applications such as aerodynamic extrusion, material processing, glass fiber and wire drawings, cooling of metallic sheets, cooling of nuclear reactors, crude oil extraction and petroleum processes, passive solar systems designs among many others [2]. In practice, it has been confirmed that free convection induces the thermal stresses which promotes critical structural damage in the piping systems of nuclear reactors [3] and seabed crude oil extractions at high temperature and pressure. When a surface is continuously moving through an otherwise still medium, boundary-layer always ensues. This mechanism finds applications in manufacturing and materials processes such as aerodynamic plastic and paper productions, hot rolling, metal casting, glass fiber production, wire drawing and spinning, and crystal growing [4]. The pioneering work on an incompressible steady boundary-layer flow and heat transfer past a linearly stretching plate was examined theoretically [5]. The researchers [5, 6] extended the work of Crane on steady free convective problem of stretching sheet under different physical situations and boundary conditions. Several studies are ongoing for use of Lie symmetry in solving heat and mass transfer not only in Newtonian but also non-Newtonian fluid flow past stretching surfaces. More recently [7] and his research colleagues employed multiple symmetry analysis as per expanding sheet in a Casson fluid.
Thermal radiation effects become relevant when the temperature difference between the fluid and the solid surface are considerably high. Immediate applications are in engineering and geophysics most especially in space technology, high temperature processes and geothermal systems [3, 8].
To predict the fluid flow behavior correctly, it is necessary to put into account the viscosity variation of an incompressible fluid which in practice is temperature dependent. Of course, the fluid temperature is itself dependent on the spatial coordinates. The viscosity of a fluid is generally

IJMSO
International Journal of Mathematical Sciences and Optimization: Theory and Applications
Vol. 9, No. 1, pp. 59 - 80
https://doi.org/10.5281/zenodo.8218009

dependent on temperature and pressure. For gases it increases rapidly with temperature, but decreases with increase in temperature for common liquids such as water, light and crude oils. For example, experimental results indicate that at room temperature of about 200 C, a one percent change in temperature proffers a seven percent change in the water viscosity and approximately a twenty six percent change in the glycerol viscosity [9].

Active research in momentum, mass and heat transfer in porous medium has received increasingly large-scale attention in the literature during the past recent decades in view of the relevance of the topic in technological devices and applications [10]. Most often it is necessary to introduce porous matrix into the flow regime of boundary layer flow as this may serve as a means of reducing the speed which consequently dampens the influence of boundary layer separation or postpone transition from laminar to turbulence flow. Flows through porous media have many applications in several engineering devices and industrial processes such as design of heat exchangers, chemical devices and process equipment, industrial filtrations, underground water pollution control, storage of nuclear wastes and many others.

The method of scaling group of transformations finds its source from the symmetries associated with some classes of differential equations in conjunction with auxiliary conditions under the application of classical approach of Lie group symmetries [11]. It competes favorably with the existing similarity transformations vis-à-vis, Blasius, Pouhlhausen, Boltzmann and ordinary scaling schemes. Worthy to mention is the interest in similarity solutions which stems naturally from the basic fact of provision of intermediate asymptotic solutions that possess bearings to more related complex non-similar solutions. Scaling group of transformations also possesses the property of reducing the number of the independent variables of partial differential equations by at least one [12,13]. Symmetry group of transformations in utilization has been able to preserve a system of equations along with the prescribed boundary conditions. [14] examined by means of Lie symmetry analysis the influence of Lorentz force and heat generation on boundary layer flow past a stretching sheet embedded in a porous Newtonian fluid in the presence of variable viscosity. Their findings reveal that heat generation and the magnetic field can reduce the boundary layer thickness. Lie group algebra has been successfully employed to solve problem of flow and heat transfer of a non-Newtonian hyperbolic tangent MHD fluid flow in the periphery of a uniformly heated stretching plate [15]. They sorted for numerical solution through MATHEMATICA-10 software package. Many authors employed one or two-parameter group of transformation to tackle some fluid dynamical problems. The mechanism of two-parameter groups reduces the number of independent variables of PDEs by two [16,45]. The methodology of solution is dependent on the auxiliary equations which are much easy and straightforward ways for obtaining similarity solutions.

Transfer of heat by free convection in a boundary-layer laminar flow has been analyzed on large scale for isothermally, non-isothermally or convectively heated plate [12,13] without much deserved attention to surfaces subjected to uniform or prescribed wall heating in the presence of thermal radiation. Heating by utilizing electromagnetic wave devices such as microwave ovens, induction furnaces, hairdryers, among others can serve as means of providing prescribed heat flux at the walls of processed materials and food products of which temperature controls are essentially important as in most agro-engineering and industrial processes such as material drying of the ultimate products or produce for storage of grains and dried vegetable animal feeds. Several learned articles under various physical aspects with uniform or prescribed surface heat flux have been reported in recent years [14–16].

A large number of practical technological applications involving natural convective flow and heat transfer in the presence of fluid withdrawal (suction) or mass blowing (injection) through a continuously moving surface has increased in the recent years. An example is in the seabed extraction of enhanced thermal recovery of crude oil. Suction can be applied for removal of reactants in chemical processes. In contrast, injection can be used to add reactants [17]. In problems of convection concerning shrinking of surfaces, lateral mass flux is needed as to curtail the influence of boundary layer separation and confine the vorticity generated within the thin layer for sustenance of the boundary layer structure [18].

In the respected journals, hundreds of scientific articles have been written on various physical as-

IJMSO

International Journal of Mathematical Sciences and Optimization: Theory and Applications
Vol. 9, No. 1, pp. 59 - 80
https://doi.org/10.5281/zenodo.8218009

pects of boundary-layer flow and heat transfer to analyze the effects of surface stretching. The work of [19–21] is among a few of the typical inclusions. Little attention has been paid to the case of shrinking effects in spite of its elaborate and widespread applications in some material processes such as shrink wraps, flexible and reticulated foams, and many others. Shrinking fluid flow is essentially associated with the backward flow induced due to the wall contraction towards a fixed point unlike the stretching fluid flow induced by surface expansion relative to a fixed point localized on the surface [22]. Some of the authors who included the effects of shrinking in their investigations [18, 23, 24].

For much closely and related allied studies of laminar forced/natural convective heat transfer from the flat surfaces analyzed through the use of Lie-group scaling of transformations, [7, 25, 26]. In the earlier studies by [27–29]; investigation was carried out on the influence of variable viscosity, thermal heat generation/absorption, uniform magnetic field or buoyancy induced flow but with unitary Grashof number for the case of isothermally heated stretching plate/sheet. However, instances in the manufacturing and materials processes involving radiation associated with surface mass flux (suction/injection), and heat transfer, very often may be dependent on application of uniform heat flux at the plate or sheet surface for proper control of quality of the final products of sheeting material moving through cooling trough [30]. A few of earlier works analyzed by means of existing similarity transformations for flow and heat transfer involving stretching sheet heating cases of (i) the surface with prescribed wall temperature and/or (ii) the surface with prescribed heat flux include [31–35].

A thorough and careful survey of literature review indicates that the present study, if extant, has not been reported. It may therefore be of interest to note that the case where the surfaces are subjected to non-uniform heat flux, and analyzed by group symmetries of transformations, which are of pertinent importance in practice lacks much needed attention. Our method of approach in line with [27, 36, 37] overrides the use of nondimensionalization through scaling analysis before the application of scaling groups of transformation as demonstrated by [38, 39].

To the best knowledge of the authors, no extant study in the literature is concerned with the combined interaction of thermal radiation, temperature-dependent viscosity and surface mass flux (suction/injection) for free convection boundary-layer flow past a non-uniformly stretching/shrinking vertical plate submitted to a variable wall heat flux and immersed in a fully saturated porous medium using one parameter Lie-group analysis. These are the crux of motivation and aim of this present investigation.

2 Model Formulation

Consider two-dimensional steady, laminar, viscous, incompressible, mixed convection boundary-layer flow of a Newtonian fluid over a semi-infinite flat plate immersed in a fully saturated porous medium as depicted in Fig. 1. The choice of coordinates (x, y) with the origin at the leading boundary-edge is such that x measured along the plate, increases in the direction parallel but opposite to the gravitational acceleration g, while y is measured normal to the plate. The fluid is quiescent with uniform ambient temperature T_∞, the permeable plate is subjected to a variable wall heat flux $q_w(x)$. Fluid velocity components along and perpendicular to the plate are $u(x, y)$ and $v(x, y)$ respectively. The mass flux normal (lateral) velocity at the wall is $V_w(x)$. The fluid confined to the region $y > 0$ is assumed to be grey, emitting and absorbing.

$$\frac{\partial u}{\partial x} + \frac{\partial \nu}{\partial y} = 0 \,, \tag{2.1}$$

$$\rho\left(u\frac{\partial u}{\partial x} + \nu\frac{\partial u}{\partial y}\right) = \frac{\partial}{\partial y}\left(\mu(T)\frac{\partial u}{\partial y}\right) + \rho g\beta(T - T_\infty) - \frac{\mu}{K_p}u \,, \tag{2.2}$$

$$(\rho C_p)\left(u\frac{\partial T}{\partial x} + \nu\frac{\partial T}{\partial y}\right) = \frac{\partial}{\partial y}\left[\left(k + \frac{16\sigma * T_\infty^3}{3k\,(k * +\sigma_s)}\right)\frac{\partial T}{\partial y}\right] \,, \tag{2.3}$$

IJMSO

International Journal of Mathematical Sciences and Optimization: Theory and Applications
Vol. 9, No. 1, pp. 59 - 80
https://doi.org/10.5281/zenodo.8218009

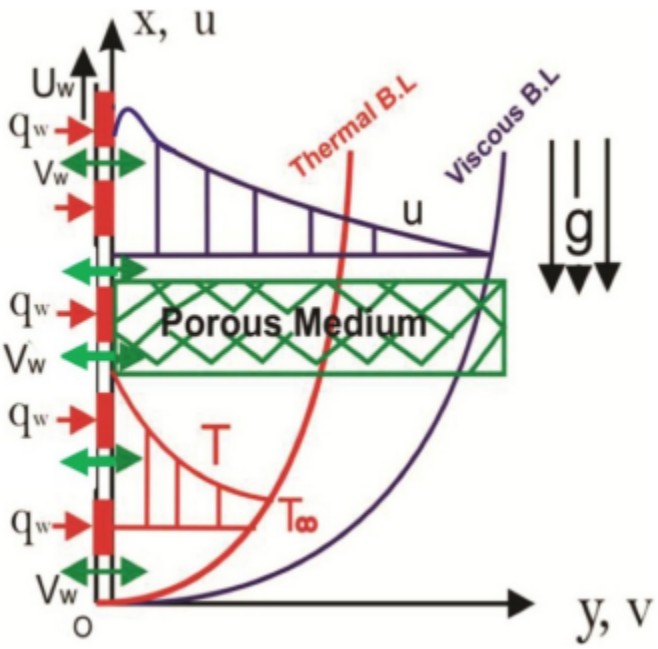

Figure 1: Schematic Diagram of the Physical Model

The boundary conditions for eqns. (1)-(3) are

$$y = 0 : u = \lambda U_w(x), \nu = V_w(x), -k\frac{\partial T}{\partial y} = q_{w0}x^n$$
$$y \to \infty : u = 0, T \to T_\infty \quad , \tag{2.4}$$

where $U_w = cx^m$, $V_w = V_0 x^{\frac{m-1}{2}}$, and $c > 0$, m, V_0 are constants. $\beta, C_p, K_p, k, k*, \sigma_s$ are respectively the thermal expansion volumetric coefficient, specific heat capacity at constant pressure, porous medium permeability coefficient, thermal conductivity coefficient, Rosseland mean absorption coefficient, Stefan-Boltzmann constant and the emission scattering coefficient. σ_s vanishes for non-scattering medium as in the present situation. Our boundary conditions for the velocity at the wall are similar to those of [45], save the sign as per the lateral velocity. It is customary to introduce stream and dimensionless temperature functions $\psi(x, y), \theta(x, y)$ as

$$u = \frac{\partial \psi}{\partial y}, \nu = -\frac{\partial \psi}{\partial x}, \theta = \frac{T - T_\infty}{\Delta T}, \Delta T = \frac{q_w}{k}\sqrt{\frac{\nu_\infty}{c}} \tag{2.5}$$

and the temperature dependent dynamic viscosity takes the form [9, 40]:

$$\mu = \mu_\infty \left[a + b\left(T_0 - T\right)\right] \tag{2.6}$$

where $T_0 \left(= \Delta T + T_\infty\right)$ is the typical temperature; $q_{w0} \neq 0$, a, b are constants such that $b = 0$ is the case for non-varying viscosity, $b > 0$ corresponds to heated wall in consequence of variable surface heat flux $q_w \left(= q_{w0}x^n\right)$ [3, 41]; $b > 0$ corresponds to cooled wall while $\mu_\infty = \mu(T_\infty)$ and $\nu_\infty = \frac{\mu_\infty}{\rho}$ are respectively the free stream viscosity and kinematic viscosity, and n is the heat flux exponent, where $n = 0$ corresponds to uniform heat flux. It is worthy to mention that the insertion of $T_\infty = 0$ into (5) recovers similar dimensionless temperature employed by [17].

IJMSO

International Journal of Mathematical Sciences and Optimization: Theory and Applications
Vol. 9, No. 1, pp. 59 - 80
https://doi.org/10.5281/zenodo.8218009

Inserting (5) into the momentum equation (2) and then into the energy equationn (3) after substituting (4) and (6), the following set of equations are obtained.

$$\begin{aligned}\frac{\partial\psi}{\partial y}\frac{\partial^2\psi}{\partial x\partial y}-\frac{\partial\psi}{\partial y}\frac{\partial^2\psi}{\partial y^2}&=-A\nu_\infty\frac{\partial\theta}{\partial y}\frac{\partial^2\psi}{\partial y^2}+\nu_\infty\left[a+A(1-\theta)\right]\frac{\partial^3\psi}{\partial y^3}\\&-\frac{\nu_\infty}{K_p}\left[a+A(1-\theta)\right]\frac{\partial\psi}{\partial y}+A\frac{g\beta}{b}\theta\end{aligned}\tag{2.7}$$

$$\frac{n}{x}\theta\frac{\partial\psi}{\partial y}+\frac{\partial\psi}{\partial y}\frac{\partial\theta}{\partial x}-\frac{\partial\psi}{\partial x}\frac{\partial\theta}{\partial y}=\frac{\nu_\infty}{Pr}(1+Nr)\frac{\partial^2\theta}{\partial y^2}\tag{2.8}$$

Also using (5) in the boundary conditions (4):

$$\left.\begin{aligned}y=0:\frac{\partial\psi}{\partial y}=\lambda cx^m,\frac{\partial\psi}{\partial x}=-V_0x^{\frac{m-1}{2}},\frac{\partial\theta}{\partial y}=-sqrt\frac{c}{\nu_\infty}\\y\to\infty:\frac{\partial\psi}{\partial y}\to0,\theta\to0.\end{aligned}\right\}\tag{2.9}$$

where $\nu_\infty=\frac{\mu_\infty}{\rho},A=b\Delta T,Pr=\frac{\mu_\infty C_p}{k}$, and $Nr=\frac{16\sigma*T_\infty^3}{3kk*}$ are respectively kinematic viscosity far from the sheet, viscosity variation parameter, the Prandtl number and the thermal radiation parameter. Note that in (8) use has been made of the relation $\frac{k_\infty}{\rho C_p}=\frac{\nu_\infty}{Pr}$.

3 Solution Method

The crux upon which the similarity solution rests, is centered on the use of a one-parameter scaling group of transformations which reduce the system of the BVPs (7)-(9) to a set of ODEs with the boundary conditions dependent on only one independent variable referred to as similarity variable. 3.1 Lie-group analysis Introduce the following simple form of one-parameter Lie-group transformation [27]:

$$\Gamma=\left\{\begin{array}{l}x^*=xe^{\dot{U}\alpha_1},y^*=ye^{\dot{U}\alpha_2},\psi^*=\psi e^{\dot{U}\alpha_3},\\u^*=ue^{\dot{U}\alpha_4},\nu^*=\nu e^{\dot{U}\alpha_5},\theta^*=\theta e^{\dot{U}\alpha_6}\end{array}\right.\tag{3.1}$$

where $\dot{U}$ is a small parameter and $\alpha_i,i=1to6$ are arbitrary transformation parameters. The preceding equation (10) depicts Γ as a point transformation of coordinates (x,y,ψ,u,ν,θ) to new coordinates $(x*,y*,\psi*,u*,\nu*,\theta*)$. Applying (10) on equations (7)-(9), the following system of equations are obtained:

$$\begin{aligned}e^{\epsilon(\alpha_1+2\alpha_2-2\alpha_3)}\left\{\frac{\partial\psi^*}{\partial y^*}\frac{\partial^2\psi^*}{\partial x^*\partial y^*}-\frac{\partial\psi^*}{\partial x^*}\frac{\partial^2\psi^*}{\partial y^{*2}}\right\}&=-A\nu_\infty e^{\epsilon(3\alpha_2-\alpha_3-\alpha_6)}\frac{\partial\theta^*}{\partial y^*}\frac{\partial^2\psi^*}{\partial y^{*2}}\\+\nu_\infty\left(a+A\right)e^{\epsilon(3\alpha_2-\alpha_3)}\frac{\partial^3\psi^*}{\partial y^{*3}}&-A\nu_\infty\theta^*e^{\epsilon(3\alpha_2-\alpha_3-\alpha_6)}\frac{\partial^3\psi^*}{\partial y^{*3}}\\-\frac{\nu_\infty}{K_p}\left[a+A\left(1-\theta^*e^{-\epsilon\alpha_6}\right)\right]e^{\epsilon(\alpha_2-\alpha_3)}\frac{\partial\psi^*}{\partial y^*}&+\frac{A}{b}g\beta\theta^*e^{-\epsilon\alpha_6}\end{aligned}\tag{3.2}$$

$$\begin{aligned}e^{\epsilon(\alpha_1+\alpha_2-\alpha_3-\alpha_6)}\left\{nx^{*-1}\theta^*\frac{\partial\psi^*}{\partial y^*}+\frac{\partial\psi^*}{\partial y^*}\frac{\partial\theta^*}{\partial x^*}-\frac{\partial\psi^*}{\partial x^*}\frac{\partial\theta^*}{\partial y^*}\right\}\\=\frac{\nu_\infty}{Pr}(1+Nr)e^{\epsilon(2\alpha_2-\alpha_6)}\frac{\partial^2\theta^*}{\partial y^{*2}}\end{aligned}\tag{3.3}$$

$$\begin{aligned}y^*e^{-\epsilon\alpha_2}=0:e^{\epsilon(\alpha_2-\alpha_3)}\frac{\partial\psi^*}{\partial y^*}=\sigma u^*e^{-\dot{U}\alpha_4}\equiv\sigma cx^{*m}e^{-m\dot{U}\alpha_1},\\e^{\epsilon(\alpha_1-\alpha_3)}\frac{\partial\psi^*}{\partial x^*}=-V_0x^{*\frac{m-1}{2}}e^{-\epsilon\alpha_5},e^{\epsilon(\alpha_2-\alpha_6)}\frac{\partial\theta^*}{\partial y^*}=-\sqrt{\frac{c}{\nu_\infty}}.\end{aligned}\tag{3.4}$$

IJMSO

International Journal of Mathematical Sciences and Optimization: Theory and Applications
Vol. 9, No. 1, pp. 59 - 80
https://doi.org/10.5281/zenodo.8218009

From (11), comparing exponents:

$$\alpha_1 + 2\alpha_2 - 2\alpha_3 = 3\alpha_2 - \alpha_3 - \alpha_6 = 3\alpha_2 - \alpha_3 = \alpha_2 - \alpha_3 - \alpha_6 = \alpha_2 - \alpha_3 = -\alpha_6 \tag{3.5}$$

From (12), comparing exponents:

$$\alpha_1 + \alpha_2 - \alpha_3 = 2\alpha_2 - \alpha_6 \tag{3.6}$$

From (13), comparing exponents:

$$\alpha_2 - \alpha_3 \equiv -\alpha_4 \equiv -\alpha_1, \alpha_1 - \alpha_3 \equiv -\alpha_5 \tag{3.7}$$

Relations (14)-(16) yield

$$\alpha_6 = 0, \alpha_1 = \alpha_1, \alpha_2 = \frac{1}{4}\alpha_1, \alpha_3 = \frac{3}{4}\alpha_1, \alpha_4 = \frac{1}{2}\alpha_1, \alpha_5 = -\frac{1}{4}\alpha_1; m = \frac{1}{2} \tag{3.8}$$

It is noteworthy to mention that the solution parameters were selected and sorted out in compliance with the invariance of the transformations. Additionally, we realize that the use of symmetry reduction, naturally renders the existence condition $n = 2m - 1$ invariantly neutral here [42]. However, the special case for which $n = 0$ corresponds to natural convection driven by a uniform heat flux.
Using (17) in (10), the system of transformations is reduced to the following new system with one group parameter:

$$\Gamma^* : \begin{cases} x^* = xe^{\dot{U}\alpha_1}, y^* = ye^{\dot{U}\frac{\alpha_1}{4}}, \psi^* = \psi e^{\dot{U}\frac{3\alpha_1}{4}}, \\ u^* = ue^{\dot{U}\frac{\alpha_1}{2}}, \nu^* = \nu e^{\dot{U}\frac{\alpha_1}{4}}, \theta^* = \theta \end{cases} \tag{3.9}$$

Expanding (18) by Lagrange's theorem of the mean, we obtain

$$x^* = x + x\epsilon\alpha_1, y^* = y + y\frac{\alpha_1}{4}\epsilon, \psi^* = \psi + \psi\epsilon\frac{3\alpha_1}{4}, u^* = u + u\epsilon\frac{\alpha_1}{2},$$

$$\nu^* = \nu - \nu\epsilon\frac{\alpha_1}{4}, \theta^* = \theta \tag{3.10}$$

with auxiliary equations

$$\frac{dx}{\alpha_1 x} = \frac{4dy}{\alpha_1 y} = \frac{4d\psi}{3\alpha_1\psi} = \frac{2du}{\alpha_1 u} = -\frac{4d\nu}{\alpha_1\nu} = \frac{d\theta}{0} \tag{3.11}$$

together with the corresponding functional invariant solutions taking the form:

$$\eta = x^{-\frac{1}{4}}y, \psi = x^{\frac{3}{4}}F(\eta), \theta = \theta(\eta) \tag{3.12}$$

The relation (21) satisfies automatically the continuity equation (1), while the momentum, energy, and the boundary conditions transform invariantly as

$$\frac{1}{2}F'^2 - \frac{3}{4}FF'' = -A\nu_\infty\theta'F'' + \nu_\infty\left(a + A - A\theta\right)F'''$$

$$-\frac{\nu_\infty}{K_p}\left(a + A - A\theta\right)F' + AGrc^2\theta \tag{3.13}$$

$$n\theta F' - \frac{3}{4}F\theta' = \frac{\nu_\infty}{Pr}\left(1 + Nr\right)\theta'' \tag{3.14}$$

$$\left.\begin{aligned} F'(0) = c\lambda, F(0) = \tfrac{3}{4}V_0, \theta'(0) = -\sqrt{\tfrac{c}{\nu_\infty}} \\ F'(\infty) = 0, \theta(\infty) = 0 \end{aligned}\right\} \tag{3.15}$$

IJMSO
International Journal of Mathematical Sciences and Optimization: Theory and Applications
Vol. 9, No. 1, pp. 59 - 80
https://doi.org/10.5281/zenodo.8218009

where primes denote ordinary differentiation with respect to η, $Fw = -\frac{4}{3}V_0$ is the suction/injection parameter $Fw = 0$ (or $Vw = 0$) indicates that the plate is impermeable, $Fw > 0$ (or $Vw < 0$) indicates suction or fluid withdrawal from the plate while $Fw < 0$ (or $Vw > 0$) indicates injection or mass blowing through the plate) . Clearly, Gr is the modified Grashof number (buoyancy parameter); exhibited as $Gr = \frac{g\beta}{b}\frac{x}{U_w^2}$. From physical point of view, $Gr = 0$ indicates the absence of natural convection, $Gr > 0$ connotes cooling of the surface, while $Gr < 0$ connotes heating of the surface.
To scale out c and ν_∞, we apply yet another transformation for η, F and θ as follows

$$\eta = \nu_\infty^{\alpha} c^{\beta} \eta^*, F = \nu_\infty^{\alpha'} c^{\beta'} F^*, \theta = \nu_\infty^{\alpha''} c^{\beta''} \Theta^*. \tag{3.16}$$

where η^*, F^*, Θ^* are variables and $\alpha, \alpha', \alpha'', \beta, \beta', \beta''$ are transformation parameters.
Applying (25) on the last set of equations (22)-(24), following similar steps as those in equations (11)-(13) and comparing exponents, we obtain

$$\alpha'' = 0, \alpha' = \frac{1}{2}; \quad \beta'' = 0, \beta' = -\beta = \frac{1}{2} \tag{3.17}$$

Use is made of relation (26) in the set of equations upon which the relation (25) was applied; and after replacement of F^*, Θ^* respectively by f, θ the following dimensionless governing equations are gotten:

$$(a + A - A\theta) f''' - A\theta' f'' + \frac{3}{4} f f'' - \frac{1}{2} f'^2 - Da\,(a + A - A\theta) f' + Gr\theta = 0 \tag{3.18}$$

$$(1 + Nr)\,\theta'' + Pr\left(\frac{3}{4} f\theta' - n\theta f'\right) = 0 \tag{3.19}$$

$$\left.\begin{aligned} f'(0) = \lambda, \quad f(0) = Fw, \quad \theta'(0) = -1 \\ f'(\infty) = 0, \quad \theta(\infty) = 0 \end{aligned}\right\} \tag{3.20}$$

3.2 Skin-friction coefficient and Nusselt number:
The physical quantities of pertinent interest are the local skin-friction coefficient Cf_x and the local Nusselt number Nu_x, which represent the wall shear stress and the heat transfer rate at the surface respectively. They may be defined as

$$Cf_x = \frac{\tau_w}{\rho U_w^2}, \quad Nu_x = \frac{x q_w}{k\,(T_w - T_\infty)}, \tag{3.21}$$

where

$$\tau_w = \mu_\infty \left[(a + A\,(1 - \theta))\,\frac{\partial u}{\partial y}\right]_{y=0}, \quad q_w = -\left[k\frac{\partial T}{\partial y} + \frac{16\sigma^* T_\infty^3}{3k^*}\frac{\partial T}{\partial y}\right]_{y=0} \tag{3.22}$$

Substituting (5) (21) and (26) into (30)-(31), the non-dimensional forms of Cf_x and Nu_x are respectively written as

$$Cf_x Re_x^{\frac{1}{2}} = (a + A\,(1 + \theta(0)))\,f''(0); \quad Nu_x Re_x^{-\frac{1}{2}} = \frac{1 + Nr}{\theta(0)}, \tag{3.23}$$

where use has been made of the condition $\theta'(0) = -1$. 3.3 Numerical simulation The set of equations (27)-(28) under the boundary conditions (29) have been solved numerically using a shooting algorithm with a fourth order Runge-Kutta-Gill integration scheme, for full detail [43]. A systematic guessing of $f''(0)$ and $\theta'(0)$ have been accessed until upstream (far-field) boundary conditions are gotten asymptotically. Use has been made of the step-size $\Delta\eta = 10^{-3}$ as per the numerical computations, ensuring the grid independent quest for optimization of our solutions with accuracy up to the seventh decimal place (10^{-7}); found to be sufficient for convergence criterion. Based on this technique, a finite value $\eta_max = 8$ has been adopted in place of $\eta \leftarrow \infty$ (in nearly all the cases) which depends on the simulated values of the physical parameters: A, Da, Gr, Pr, Nr, Fw, n and λ. Also, the computations were carried out by a program coded in a symbolic and computational computer language, Maple-18.

IJMSO

International Journal of Mathematical Sciences and Optimization: Theory and Applications
Vol. 9, No. 1, pp. 59 - 80
https://doi.org/10.5281/zenodo.8218009

4 Results and discussion

A parametric study of the controlling physical flow parameters each with specified value 0.2 with exception of the Prandtl number which bears the value of 0.72 (for air), has been conducted as per the computation default data. Situations with different values are conspicuously demonstrated in the tabular cells for fluid characteristics (skin-coefficient and Nusselt number) or graphical legends (velocity and temperature).

4.1 Effects of parameter variation on skin-friction and Nusselt number

From the process of numerical computations, the reduced skin friction coefficient and Nusselt number, which are defined in (33) were all sorted out in terms of the velocity gradient at the wall and , the plate temperature, and their numerical values are presented in a tabular form. The accuracy of this numerical code has been accessed by direct comparison with the numerical results reported by [4, 44] as indicated in Tables 2 and 3, and found to be in satisfactory agreement. It is worthy to mention here, that in our numerical computations moderate simulated values of Prandtl numbers were administered as asymptotic behaviour for high values could not be achieved herein.

Table 4 unveils the influences of the physical flow parameters in the list: $A, Da, Gr, Pr, Nr, Fw > 0, Fw < 0, n > 0, n < 0$ and $\lambda > 0, \lambda < 0$ on the velocity gradient (the shear stress parameter) $f''(0)$, and the plate (wall) temperature $\theta(0)$. Intensification of the viscosity variation parameter A, and the Grashof number (buoyancy parameter) Gr, leads to value enhancement of $f''(0)$ and $\theta(0)$. However, increase in the porous medium permeability parameter Da, is tantamount to a decrease in $f''(0)$, but a rise in $\theta(0)$.

Table 2: Comparison of the values of the local inverse plate temperature $(\theta^{-1}(0)$, with [4, 31] in the absence of concentration when $a = 1, A = Da = Nr = 0$

	Pr								
	Ali (1995)			Elbashbeshy *(1998)*			Present work		
F w	0.72	1	10	0.72	1	10	0.72	1	10
-0.6	0.7623	1.0063	7.0923	0.77110	1.00600	7.09210	0.769086	1.007520	7.092016
-0.4	0.6563	0.8557	5.3524	0.66350	0.85540	5.35040	0.665680	0.857715	5.352334
-0.2	0.5565	0.7139	3.7334	0.56210	0.71360	3.7327	0.568921	0.717100	3.733284
0	-	-	-	0.46780	0.58210	2.30730	0.479526	0.587222	2.307567
0.1	-	-	-	0.42360	1.69920	0.52060	0.437785	0.526793	1.698916
0.2	0.3791	0.4637	1.1798	0.38150	0.46240	1.17950	0.398103	0.469617	1.178971
0.3	-	-	-	0.3416	0.4075	0.7608	0.360532	0.415858	0.759856

As can be seen in this table, both $f''(0)$ and $\theta(0)$ depreciate in magnitude in consequence of increase in the suction parameter $Fw > 0$, Prandtl number Pr, stretching parameter $\lambda < 0$ and heat flux exponent $n > 0$. Nonetheless, an increase in either of the injection parameter $Fw < 0$ radiation parameter Nr shrinking parameter $\lambda < 0$ or negative heat flux exponent $n < 0$ improves the value of velocity gradient and plate temperature. We observe in Table 4 that when $Gr = 0$, while other parameters bear fixed values (i.e. absence of natural convection) the flow is driven by stretching effect and the value of $f''(0)$ is negative. Also, for the stretching case $\lambda > 0$ with other parameters non-varying in values, the values of $f''(0)$ are negative. In physical terms, the negative values of $f''(0)$ signify that the plate impresses a drag force on the fluid while the usual positive values manifest the reverse.

4.2 Effects of parameter variation on velocity and temperature profiles

In order to gain a thorough insight into the present work, further investigations were carried out for the effects of various emerging physical parameters on the velocity and temperature fields as depicted graphically in Figures 2-18, taking $a = 1$. Generally, both the dimensionless fluid velocity $f'(\eta)$ and temperature $\theta(\eta)$ assume the plate values and vary curvilinearly away from the plate within the boundary-layer and nosedive towards the boundary-edge satisfying the free stream boundary

IJMSO

International Journal of Mathematical Sciences and Optimization: Theory and Applications
Vol. 9, No. 1, pp. 59 - 80
https://doi.org/10.5281/zenodo.8218009

Table 3: Comparison of the values of the local inverse plate temperature $(\theta^{-1}(0)$, with [31] in the absence of concentration when $\lambda = a = 1, A = Da = Nr = 0$

n	Fw	Pr					
		Elbashbeshy (1998)			Present work		
		0.72	1	10	0.72	1	10
1	-0.6	1.053	1.3437	8.0128	1.046195304	1.344644085	8.017574
1	-0.4	0.9672	1.2196	6.4226	0.962810194	1.220675105	6.425632
1	-0.2	0.8882	1.1048	4.9751	0.886024862	1.106134264	4.976043
1	0	0.8161	1.0	3.7202	0.815779908	1.001396213	3.720217
1	0.1	0.7825	0.9512	3.1816	0.783040001	0.952745535	3.181495
1	0.2	0.7505	0.905	2.7092	0.751832256	0.906560665	2.709015
1	0.3	0.7204	0.8613	2.3052	0.722105996	0.862810348	2.304829
-1	-0.6	0.4385	0.6	5.9988	0.443464	0.602826	6.000000
-1	-0.4	0.2391	0.4001	4.0000	0.305729	0.405372	4.000000
-1	-0.2	0.1483	0.2003	2.0000	0.170945	0.209974	1.999999
-1	0	0.0761	0.01005	1.0001	0.040284	0.018111	0.018111
-1	0.1	−0.0669	−0.0985	−1.0000	-0.023030	-0.075790	-0.999999
-1	0.2	−0.1378	−0.1977	−2.0000	-0.084699	-0.167812	-2.00000
-1	0.3	−0.2080	−0.2966	−3.0000	-0.144456	-0.257436	-3.00000

Table 4: Computations showing varying values of the wall velocity gradient $f''(0)$ and plate temperature $(\theta(0)$, for various values of physical flow parameters indicated when $a = 1$

Parameter	Variation	$f''(0)$	$\theta(0)$	Parameter	Variation	$f''(0)$	$\theta(0)$
A	**0**	0.212652	1.982107	**Pr**	**0.72**	0.253388	1.975798
	0.1	0.231116	1.979269		**1**	0.174268	1.732188
	0.2	0.253388	1.975798		**10**	-0.10144	0.465271
Da	**1**	0.112747	2.18712	**λ**	**-0.1**	0.686722	2.41811
	1.5	0.052899	2.28229		**-0.2**	0.845104	2.598255
	2	0.003201	2.360907		**-0.3**	1.013996	2.792956
Fw	**-0.3**	0.352487	2.349643		**0**	0.536662	2.254106
	-0.2	0.334709	2.271648		**0.1**	0.392848	2.106782
	0	0.296007	2.120582		**0.2**	0.253388	1.975798
	0.2	0.253388	1.975798	**n**	**0.3**	0.116622	1.86019
	0.3	0.23076	1.905707		**-3**	0.508929	3.416737
Gr	**0**	-0.16527	2.667947		**-2**	0.144421	2.237733
	0.2	0.253388	1.975798		**0**	0.03248	1.675061
	2	1.756651	1.413771		**2**	-0.01354	1.397567
	10	5.635997	1.153066		**3**	-0.02849	1.300024
Nr	**0**	0.208066	1.839312				
	1	0.400627	2.373053				
	3	0.654583	2.934397				
	5	0.835317	3.262193				

conditions asymptotically. Figures 2-3 demonstrate the effects of viscosity variation parameter A, on the velocity and temperature fields for either stretching or shrinking plate. It is observed that adjacent to the wall, $f'(\eta)$ increases in either of the cases of stretching or shrinking, but far away from it the opposite trend prevails. However, increase in A, leads to mild temperature fall in the

IJMSO
International Journal of Mathematical Sciences and Optimization: Theory and Applications
Vol. 9, No. 1, pp. 59 - 80
https://doi.org/10.5281/zenodo.8218009

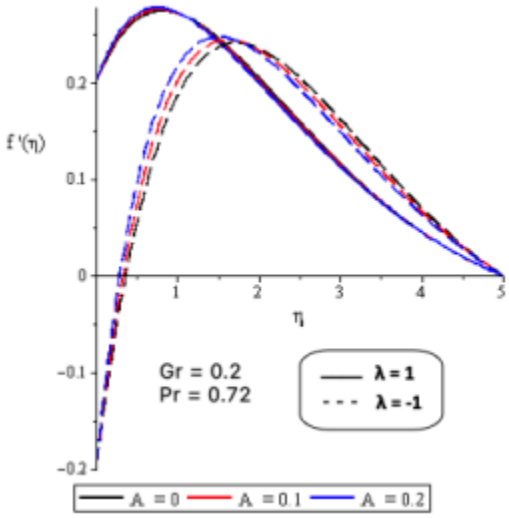

Figure 2: Variation of velocity $f'(\eta)$ for different viscosity variation parameter A.

case of stretching but strong temperature falls for a shrinking plate. The effects of porous medium permeability parameter Da, on $f'(\eta)$ and $\theta(\eta)$ are depicted in Figures 4-5. Clearly Da impedes the fluid motion and in consequence raises the temperature within the boundary layer for both stretching and shrinking cases. From these figures, it is affirmed that the viscous boundary-layer thickness depreciates while the thermal boundary-layer thickens as the porous medium parameter strengthens. The trends of responses of the fluid velocity and temperature due to increasing value of suction/injection parameter, as revealed in Figures 6-7 signal a damping influence on the velocity for both stretching and shrinking plate, and fluid temperature as in the case of stretching while the temperature of the fluid rises for a shrinking plate. Figures 8-9 unveil the effects of the buoyancy parameter Gr, on the velocity and fluid temperature for stretching/shrinking plate. As observed, the influence of increasing natural convection parameter Gr, is to accelerate the fluid and stem down the fluid temperature increasingly. Also, when $Gr = 0$ (absence of natural convection), a straight-line profile ensues, indicating a transformation to convective flow subjected to pure stretching of the plate in which the plate establishes a dragging force on the fluid (see Table 4 and discussion therein). Figures 10-11 settle the effects of the heat flux exponent n on $f'(\eta)$ and $\theta(\eta)$. As can be seen in these figures, increasing n gives rise to decrease in $f'(\eta)$ and $\theta(\eta)$ in a stretching/shrinking plate. Figures 12-13 display the varying influence of the radiation parameter on the velocity and fluid temperature within the boundary layer. These figures illustrate that, in a stretching/shrinking plate, increasing Nr causes a significant increase in $f'(\eta)$ and $\theta(\eta)$. Strengthening the Prandtl number, as illustrated in Figure 14, procures a significant increase in stretching case and a decrease in the shrinking case for the fluid velocity within the boundary layer while the fluid temperature falls drastically as predicted in Figure 15, due to increasing value of Pr in both cases of the plate motion. Figures 16-17 show the effects of stretching/shrinking parameter on the velocity and the fluid temperature when other physical parameters have fixed values. In these figures, near the plate, increase in the stretching parameter $\lambda > 0$, can accelerate the fluid and stem temperature from rising in the boundary layer while the reverse trend is predicted when the shrinking parameter $\lambda < 0$ intensifies.

IJMSO
International Journal of Mathematical Sciences and Optimization: Theory and Applications
Vol. 9, No. 1, pp. 59 - 80
https://doi.org/10.5281/zenodo.8218009

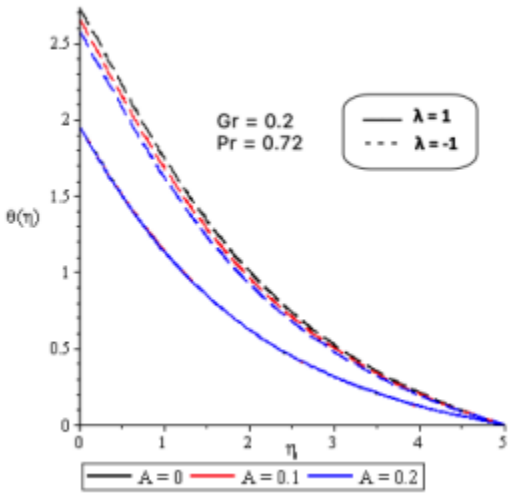

Figure 3: Temperature $\theta(\eta)$ variation for different viscosity variation parameter A.

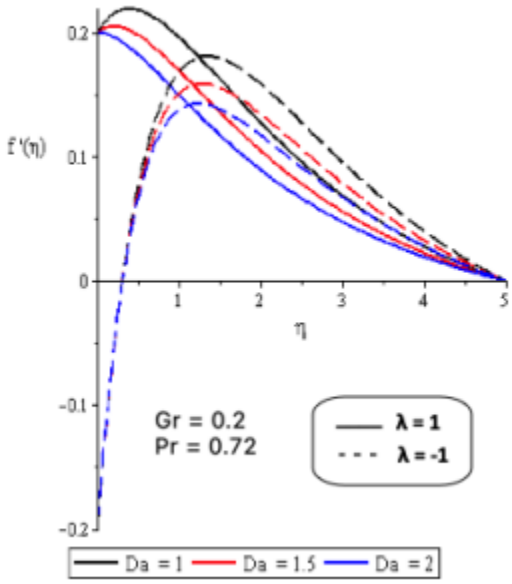

Figure 4: Variation of velocity $f'(\eta)$ for different permeability parameter Da.

IJMSO
International Journal of Mathematical Sciences and Optimization: Theory and Applications
Vol. 9, No. 1, pp. 59 - 80
https://doi.org/10.5281/zenodo.8218009

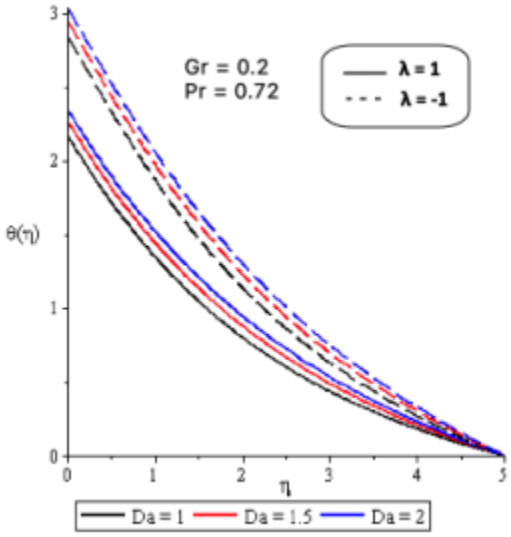

Figure 5: Temperature $\theta(\eta)$ variation for different permeability parameter Da.

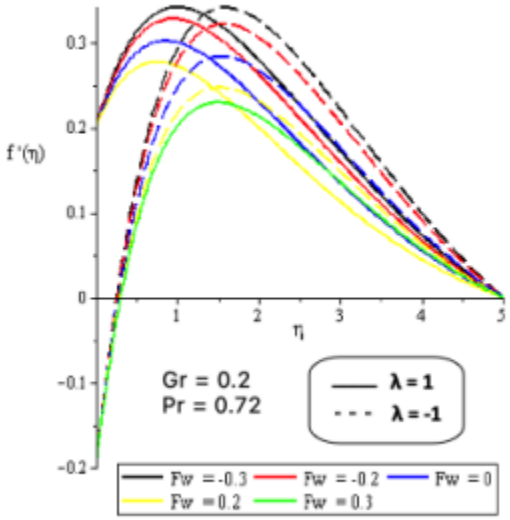

Figure 6: Variation of velocity $f'(\eta)$ for different suction parameter Fw.

IJMSO
International Journal of Mathematical Sciences and Optimization: Theory and Applications
Vol. 9, No. 1, pp. 59 - 80
https://doi.org/10.5281/zenodo.8218009

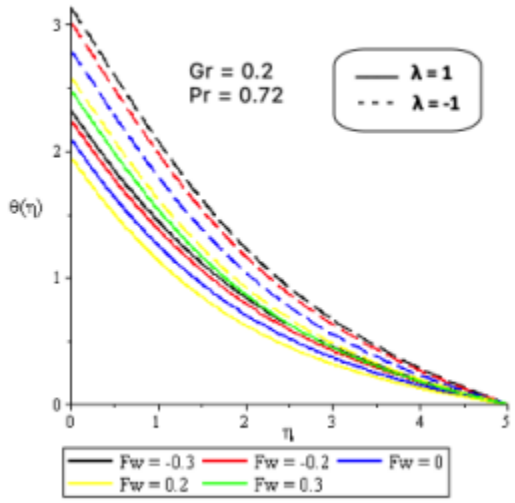

Figure 7: Temperature $\theta(\eta)$ variation for different suction parameter Fw.

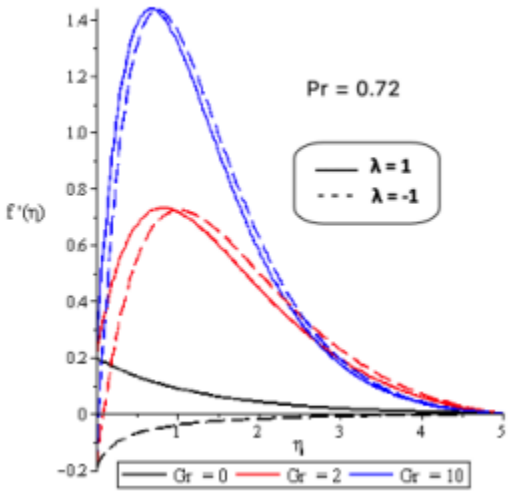

Figure 8: Variation of velocity $f'(\eta)$ for different Grashof number Gr.

IJMSO
International Journal of Mathematical Sciences and Optimization: Theory and Applications
Vol. 9, No. 1, pp. 59 - 80
https://doi.org/10.5281/zenodo.8218009

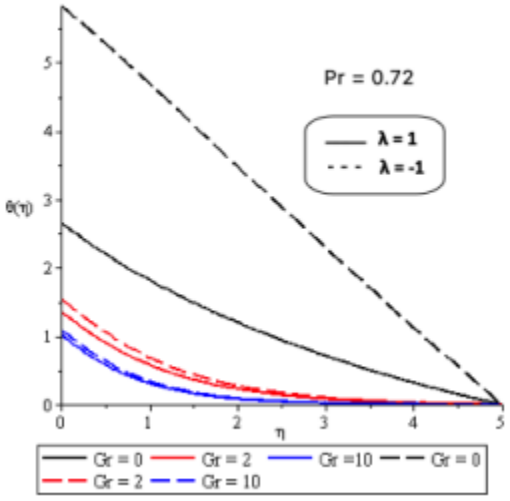

Figure 9: Temperature $\theta(\eta)$ variation for different Grashof number Gr.

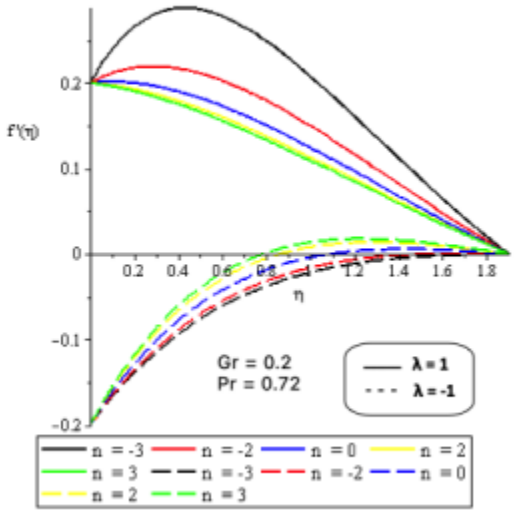

Figure 10: Variation of velocity $f'(\eta)$ for different heat flux exponent n.

IJMSO

International Journal of Mathematical Sciences and Optimization: Theory and Applications
Vol. 9, No. 1, pp. 59 - 80
https://doi.org/10.5281/zenodo.8218009

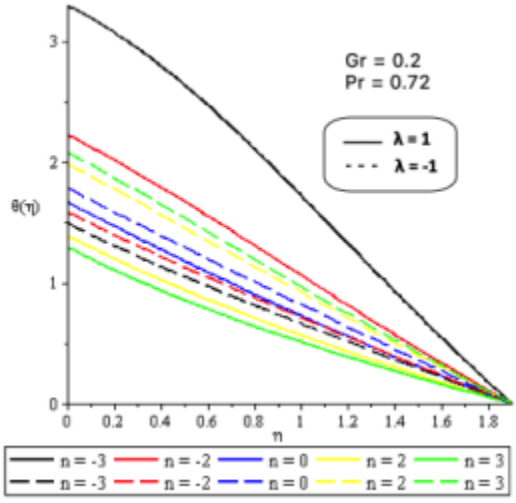

Figure 11: Temperature $\theta(\eta)$ variation for different heat flux exponent n.

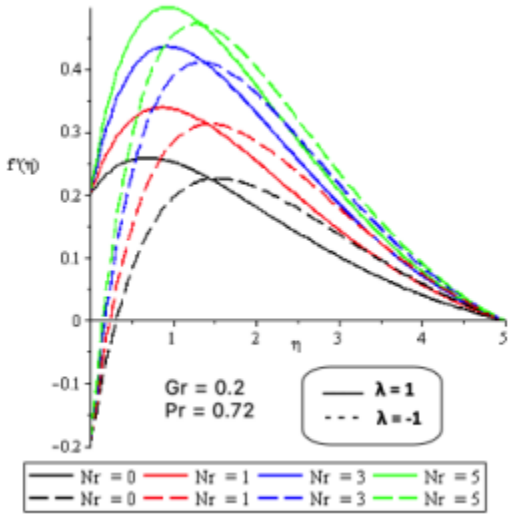

Figure 12: Variation of velocity $f'(\eta)$ for different thermal radiation parameter Nr.

IJMSO

International Journal of Mathematical Sciences and Optimization: Theory and Applications
Vol. 9, No. 1, pp. 59 - 80
https://doi.org/10.5281/zenodo.8218009

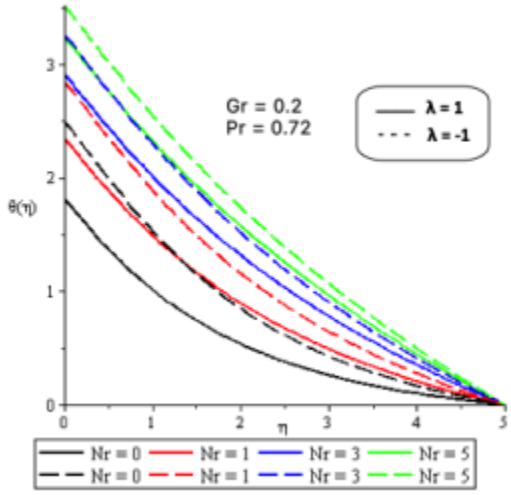

Figure 13: Temperature $\theta(\eta)$ variation for different thermal radiation parameter Nr.

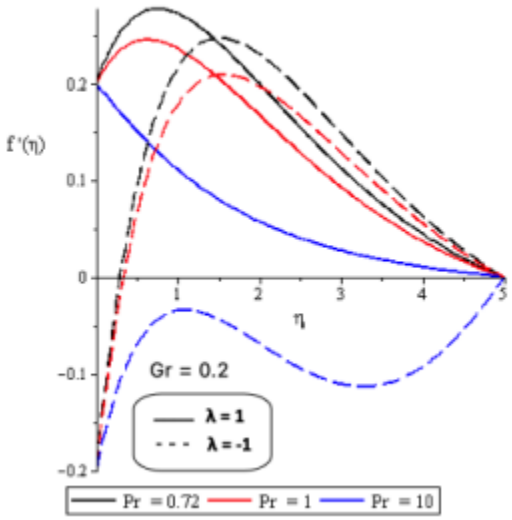

Figure 14: Variation of velocity $f'(\eta)$ for different Prandtl number Pr.

IJMSO
International Journal of Mathematical Sciences and Optimization: Theory and Applications
Vol. 9, No. 1, pp. 59 - 80
https://doi.org/10.5281/zenodo.8218009

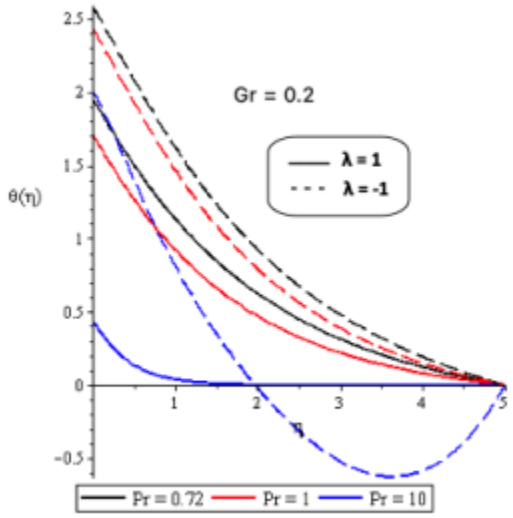

Figure 15: Temperature $\theta(\eta)$ variation for different Prandtl number Pr.

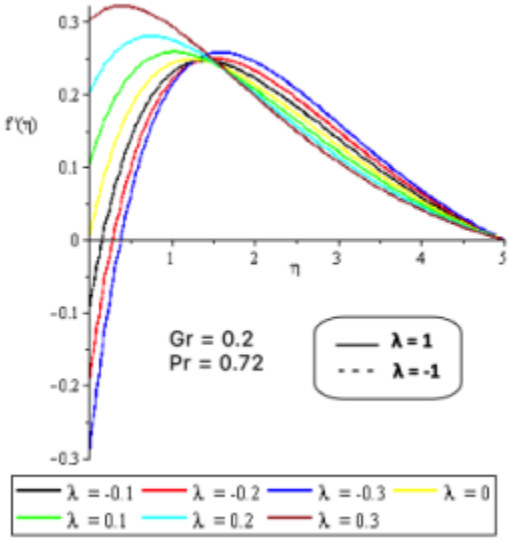

Figure 16: Variation of velocity $f'(\eta)$ for different stretching parameter λ.

IJMSO

International Journal of Mathematical Sciences and Optimization: Theory and Applications
Vol. 9, No. 1, pp. 59 - 80
https://doi.org/10.5281/zenodo.8218009

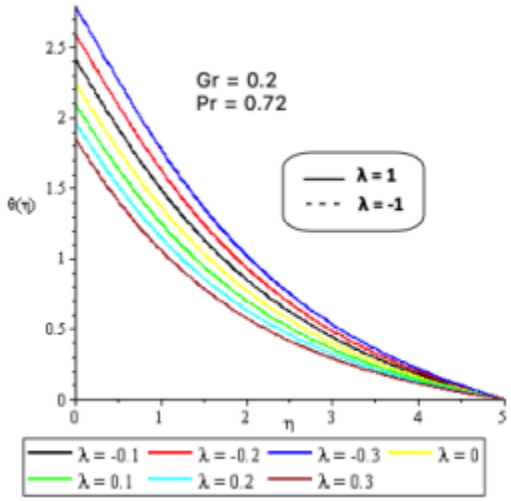

Figure 17: Temperature $\theta(\eta)$ variation for different stretching parameter λ.

5 Conclusion

The major findings of this study are itemised as follows:

- The surface shear stress parameter and plate temperature are higher in values due to injection as compared with those due to suction insofar as the plate stretches.
- The porous medium parameter impedes the fluid motion and in consequence raises the plate temperature for stretching or shrinking surface.
- The surface shear stress parameter is significantly enhanced whereas, not only the plate temperature but also the entirety of the fluid temperature falls as the radiation parameter intensifies for stretching/shrinking plate motion.
- The enhancement of shrinking parameter decelerates the fluid, and in consequence raises the plate temperature considerably.
- Viscosity variation parameter can cause a rise in the fluid velocity and a fall in plate temperature with a subsequent intensification in the value of the surface shear stress parameter.
- The influence of increasing the buoyancy parameter is to accelerate the fluid, enhance the surface shear stress parameter and stem down wall temperature in either stretching or shrinking wall motion.
- For a stretching plate, the surface shear stress parameter as well as the plate temperature depreciates in value as the Prandtl number increases.

6 Acknowledgments

The authors of this paper appreciate the efforts of the reviewers of the paper in taking out time to read through and make observations that has enriched this study. Your contributions have further advanced the annals of research. Thank you.

IJMSO

International Journal of Mathematical Sciences and Optimization: Theory and Applications
Vol. 9, No. 1, pp. 59 - 80
https://doi.org/10.5281/zenodo.8218009

References

[1] Ostrach, S. Laminar Natural Convection Flow and Heat Transfer of Fluid with and without Heat Source in Channels with Constant Wall Temperature. NACA TN 2863, (1952).

[2] Crepeau, J. C. and Clarksean, R. Similarity solutions of natural convection with internal heat generation, Transactions of ASME- Journal of Heat Transfer, 119: 183-185, (1997).

[3] Pop, I. and Ingham, D. B. Convective heat transfer: mathematical and computational modelling of viscous fluids and porous media, Elsevier Sc. & Tech. Books, US, (2001).

[4] Ali, M. E. On thermal boundary layer on a power-law stretched surface with suction or injection, Int. J. Heat and Fluid Flow, 16: 280-290, (1995).

[5] Crane, L. J. Flow past a stretching plate. Journal of Appl. Math. and Phys. (ZAMP), 21 (4), 645-647, (1970).

[6] Mukhopadhyay, S. Slip effects on MHD boundary layer flow over an exponentially stretching sheet with suction/blowing and thermal radiation, Ain Shams Engineering Journal, 4: 485-491, (2013).

[7] Safdar, M., Taj, S., Bilal, M., Ahmed, S., Khan, M. I., Moussa, S. B. Fadhl, B. M., Makhdoum, B. M., Eldin, S. M. Multiple Lie symmetry solutions for effects of viscous on magnetohydrodynamic flow and heat transfer in non-Newtonian thin film, Open Physics 2023, 21:20220244, (2023).

[8] Lee, J., Kandaswamy, P., Bhuvaneswari, M. and Sivasankaran, S. Lie group analysis of radiation natural convection heat transfer past an inclined porous surface, J. Mechanical Sci. and Tech., 22: 1779-1784, (2008).

[9] Sahin, A. Z. Second law analysis of laminar viscous flow through a duct subjected to constant wall temperature, J. Heat Transfer, 20: 76-83, (1998).

[10] Vafai, K. Handbook of porous media, 2nd Ed., Taylor & Francis Group, LLC, New York, (2005).

[11] Bluman George, Cheviakov Alexei and Anco Stephen Applications of Symmetry Methods to Partial Differential Equations, Applied Mathematical Sciences, Volume 168, Springer-Verlag New York, (2010).

[12] Uddin, Md. J., Hamad, M. A. A. and Ismail, A. I. Md. Investigation of heat mass transfer for combined slips flow: A Lie group analysis, Sains Malaysiana, 41 (9): 1139-1148, (2012).

[13] Aziz, F., El Achaby, M., Lissaneddine, A., Aziz, K., Ouazzani, N., Mamouni, R., & Mandi, L. Composites with alginate beads: A novel design of nano-adsorbents impregnation for large-scale continuous flow wastewater treatment pilots. Saudi Journal of Biological Sciences, 27(10), 2499-2508, (2020).

[14] Agrawal, P., Dadheech, P. K., Jat, R.N., Bohrab, M., Nisar, K. S and Khan, I. Lie similarity analysis of MHD flow past a stretching surface embedded in porous medium along with imposed heat source/sink and variable viscosity, jmaterrestechnol.2020;9(x x):10045–10053, (2020).

[15] Zeb, S., Khan, S., Ullah, Z., Yousaf, M., Khan, I., Alshammari, N., Alam, N. and Hamadneh, N. N. Lie Group Analysis of Double Diffusive MHDTangent Hyperbolic Flow over a Stretching Sheet, Mathematical Problems in Engineering Mathematical Problems in Engineering Volume 2022, Article ID 9919073, 14 pages https://doi.org/10.1155/2022/9919073, (2022).

[16] Abd-El-Malek, M. B., Boutros, Y. Z. and Badran, N. A. Group method analysis of unsteady free-convective laminar boundary-layer flow on a nonisothermal vertical flat plate, J. of Eng. Math., 24: 343-368, (1990).

[17] Mandal, I. C. and Mukhopadhyay, S. Heat transfer analysis for fluid flow over an exponentially stretching porous sheet with surface heat flux in porous medium, Ain Shams Engineering Journal, 4, 103-110, (2013).

[18] Bhattacharyya, K. and Pop, I. MHD Boundary layer flow due to an exponentially shrinking sheet, Magnetohydrodynamics, 47 (4): 337-344, (2011).

[19] Dutta, B. K. and Gupta, A. S. Cooling of a stretching sheet in a viscous flow, Ind. Eng. Chem. Res., 26: 333-336, (1987).

[20] Chen, C. & Char, M. Heat transfer of a continuous, stretching surface with suction or blowing, J. of Mathematical Analysis and Applications, 135, 568-580, (1988).

[21] Vajravelu, K. and Hadjinicolauo, A. Heat transfer in a viscous fluid over a stretching sheet with viscous dissipation and internal heat generation, Int. Comm. Heat and Mass Transfer, 20: 417-430, (1993).

[22] Mondal, S., Haroun, N. H. and Sibanda, P. The effects of thermal radiation on an unsteady MHD axisymmetric stagnation-point flow over a shrinking sheet in presence of temperature dependent thermal conductivity with Navier slip, PLos ONE, 10 (9): 1-23, (2015).

[23] Andersson, H. I., Hansen, O. R. and Holmedal, B. Diffusion of chemically reactive species from a stretching sheet, Int. J. Heat Mass Transfer, 37 (4): 659-664, (1994).

[24] Elbashbeshy, E. M. A. Radiation effect on heat transfer over a stretching surface, Can. J. Phys. 78: 1107–1112, (2000).

[25] Adeniyan, A. and Adigun, J. A. Similarity solution of hydromagnetic flow and heat transfer past an exponentially stretching permeable vertical sheet with viscous dissipation, Joulean and viscous heating effects, Annals of Faculty Engineering Hunedoara-Int. J. of Engineering, 14 (2): 113-120, (2016).

[26] Grubka, L. J. and Bobba, K. M. Heat transfer characteristics of a continuous, stretching surface with variable temperature, Transactions of ASME J. Heat Transfer, 107, 248-250, (1985).

[27] Mukhopadhyay, S., Layek, G. C. and Samad, S. K Study of MHD boundary layer flow over a heated stretching sheet with variable viscosity, International Journal of Heat and Mass Transfer, 48, 4460-4466, (2005).

[28] Mukhopadhyay, S. and Layek, G. C Effects of thermal radiation and variable fluid viscosity on free convective flow and heat transfer past a porous stretching surface, International Journal of Heat and Mass Transfer, 55, 2167-2178, (2008).

[29] Mukhopadhyay, S. and Layek, G. K Effects of variable fluid viscosity on flow past a heated stretching sheet embedded in a porous medium in presence of heat source/sink, Meccanica, 47 (4): 863–876, (2012).

[30] Dutta, B. K., Roy, P. and Gupta, A. S. Temperature field in flow over a stretching sheet with uniform heat flux, Int. Comm. Heat Mass Transfer,12: 89-94, (1985).

[31] Elbashbeshy, E. M. A. Heat transfer over a stretching surface with variable surface heat flux, J. Phys. D: Appl. Phys. 31: 1951–1954, (1998).

[32] Elbashbeshy, E. M. A., Yassmin, D. M. and Dalia, A. A. Heat transfer over an unsteady porous stretching surface embedded in a porous medium with variable heat flux in the presence of heat source or sink, African J. of Math. and Computer Sci. Res., 3 (6): 68-73, (2010).

[33] Miklavcic, M. and Wang, C. Y. Viscous flow due to a shrinking sheet, Quarterly of Appl. Math., 64 (2): 283-290, (2006).

[34] Fang, T., Zhang, J. and Yao, S. Viscous Flow over an Unsteady Shrinking Sheet with Mass Transfer, Chin. Phys. Lett., 26 (1): 014703 (1-4), (2009).

[35] Ali, F. Md., Nazar, R. and Arifin, N. Md. MHD viscous flow and heat transfer due to a permeable shrinking sheet with prescribed surface heat flux, Proceedings of the 9th WSEAS International conference on applications of computer engineering, 260-263, (2010).

[36] Layek, G. C., Mukhopadhyay, S. and Samad, Sk. A. Heat and mass transfer analysis for boundary layer stagnation-point flow towards a heated porous stretching sheet with heat absorption/generation and suction/blowing, International Communications in Heat and Mass Transfer, 34: 347–356, (2007).

[37] Dessie, H and Kishan, N. MHD effects on heat transfer over stretching sheet embedded in porous medium with variable viscosity, viscous dissipation and heat source/sink, Ain Shams Engineering Journal, 5, 967-977, (2014).

[38] Boutros, Y. Z., Abd-el-Malek, M. B., Badran, N. A. and Hassan, H. S. Lie-group method of solution for steady two-dimensional boundary-layer stagnation-point flow towards a heated stretching sheet placed in a porous medium, Meccanica, 41: 681-691, (2006).

[39] Hamad, M. A. A., Uddin, Md. J. and Ismail, Md. A. I. Investigation of combined heat and mass transfer by Lie group analysis with variable diffusivity taking into account hydrodynamic slip and thermal convective boundary conditions, Int. J. Heat Mass Transfer, 55: 1355-1362, (2012).

[40] Batchelor, G. K. An Introduction to Fluid Dynamics, Cambridge University Press, London, (1987).

[41] Sparrow, E. M. Analysis of laminar forced-convection heat transfer in entrance region of flat rectangular ducts (No. NACA-TN-3331), (1955).

[42] Ali, M. E. The buoyancy effects on the boundary layers induced by continuous surfaces stretched with rapidly decreasing velocities. Heat and Mass Transfer, 40(3-4), 285-291, (2004).

[43] Gill, S. A process for the step-by-step integration of differential equations in an automatic digital computing machine, Math. Proc. Cambridge Phil. Soc., 47: 96-108, (1951).

[44] Elbashbeshy, E. M. Heat transfer over a stretching surface with variable surface heat flux. Journal of Physics D: Applied Physics, 31(16), 1951, (1998).

[45] Cao, L., Si, X. Zheng, L. and Pang, H. Lie group analysis for MHD effects on the convectively heated stretching porous surface with heat source/sink, Boundary Value Problems, 63: 1-18, (2015).